

AN ALGORITHM FOR
STATISTICALLY EVALUATING RAINFALL-RUNOFF
MODEL PREDICTION PERFORMANCE

T.V. Hromadka II¹

Abstract

Given a set of realizations of error data (i.e., the difference between model runoff estimates and stream gauge data) from rainfall-runoff hydrologic models it is possible to generate a set of error transfer function realizations that, when convoluted with a suitable kernel function such as the hydrologic model output, equates to the original error data. In turn, these error transfer function realizations may be used to generate synthetic error data which is convoluted from a separate design storm modeled runoff and the generated error transfer function realizations. The synthetic error data set is then added to the design storm modeled runoff to produce a set of equally likely outcomes for the model prediction. The set of equally likely outcomes is statistically analyzed to provide, for instance, a confidence interval for the possible outcomes of the design storm model. A four section algorithm is presented which performs each of these tasks.

1 Senior Managing Engineer, Failure Analysis Associates,
4590 MacArthur Boulevard, Suite 400, Newport Beach, California 92660-2027
and Professor of Mathematics and Environmental Studies,
Department of Mathematics, California State University,
Fullerton, California 92634-9480

INTRODUCTION

The classification of rainfall-runoff hydrological models is well known in the literature. However, a uniform procedure to evaluate rainfall-runoff model performance, in prediction mode, has not been generally adopted. In this paper, an algorithm is presented that provides a means for evaluating the relative performance between rainfall-runoff model structures as applied in prediction mode. Before beginning the mathematical development a preview is presented below. As a preview of the mathematical development, let X be a random variable that we wish to estimate future outcomes. Various estimates of X are available, namely, outputs from model types Y_1, Y_2 , and so forth. We wish to compare the models Y_k as to prediction performance.

To begin, we choose one particular model Y_k , say model Y_1 . Next for m historic events, we have m ordered pairs of data $\{(x_i, y_i); i = 1, 2, \dots, m\}$ where x_i is the outcome of X for event i , and y_i is the outcome (model prediction) of Y for event i . The error for event i , for model 1, is

$$e_i = x_i - y_i.$$

For m events, there are m error values for model 1, given by the set $\{e_i; i = 1, 2, \dots, m\}$, or simply noted as the distribution of errors $[e]_1$ for model Y_1 . The error realizations $e_i = x_i - y_i$ employed to characterize the distribution of modeling error, for a particular runoff model, will be used for subsequent analysis as a sampling from a stochastic process. Inherent in this approach is the assumption that the obtained error realizations are representative of a simple random sampling of the underlying stochastic process. Additionally, the error realizations are dependent upon the runoff model used; hence, a comparison in the variance of modeling estimates can be made between model types similar to the evaluation of statistical estimators according to their respective variances. Furthermore, if sufficient data sets are available, one can partition the data according to storm size, for example, in order to investigate modeling trends with respect to storm magnitude.

Suppose we wish to predict the outcome of X , for a future event, d . Then, an estimate of X is given, for model type 1, by the distribution of values of Y_1 , for future event d , noted as $[Y]_1^d$ where

$$[Y]_1^d = y_1 + [e]_1 \quad (1)$$

where $[Y]_1^d$ is the set of m estimates for X_d from X , from model 1, for event d ; y_1 is the next outcome of Y_1 ; and $[e]_1$ is the set of historic error values, from model Y_1 .

Equation (1) can be extended to evaluation of storm runoff criterion variables (e.g., peak flow rate, peak 3-hour runoff volume, mean flow velocity for flow rates above a threshold, etc.). The subject algorithm, which is shown in Fig. 1, uses results obtained by applying the theory of stochastic integral equations (Tsokos and Padgett, 1974) to a series of actual data sets (Abbott (1978), Hromadka et al, (1987)) to determine the error realizations in each of six hydrologic models, for a set of measured rainfall-runoff storm events in an urban catchment. Each rainfall-runoff model is used to simulate, in prediction mode, four separate storm events. That is, each rainfall-runoff model was first calibrated to a set of storm data, and then the calibrated models were applied to a set of four storms that were not part of the original calibration set of storms (i.e., "validation" test runs). The six models evaluated were: 1) Continuous Flood Hydrographs (HEC-1), 2) Storm Water Management Model (SWMM), 3) Massachusetts Institute of Technology Catchment Model (MITCAT), 4) Storage Treatment Overflow Runoff Model (STORM), 5) Hydrocomp Simulation Program (HSP), and 6) Streamflow Synthesis and Reservoir Regulation (SSARR). (Descriptions of each of these models are contained in the rainfall-runoff model study prepared by Abbott, 1978).

To develop error realizations, for each particular model in prediction mode, the graphical output of each model (resulting from the validation test runs) is compared to observed stream gauge data at discrete time intervals and the difference between the two realizations is recorded as modeling error, in prediction mode, for that particular model, for the particular storm event. For use in this algorithm, the four validation storm events for each of the six models are combined in time sequence to form one large combined storm event realization, $M_k(\cdot)$, where k is the model type. The extended time frame is then divided into two-hour segments. Each two-hour segment is separated into twenty-four five minute intervals. The motivation for using two-hour segments is to synthetically develop a larger population of modeling error realizations; then a bootstrapping procedure is used to simulate random sampling. The choice of two-hour segments is based upon the hydrologic response time (i.e. time of concentration) of the study catchment being approximately one hour, and hence the central one-

hour runoff hydrograph within the two-hour segments may be mutually independent for this analysis. The error realizations are then equated to a convolution of the model output with a new transfer function called the error transfer function. By solving the inverse problem, the error transfer function realization is evolved on a two-hour time interval basis for each model structure studied.

A hypothetical storm event, called the design storm, is evaluated by convoluting the resulting design storm model output (for a chosen model type) with the set of error transfer functions that correspond to the chosen model. This generates a new set of error realizations which are subtracted with the design storm model output to create a set of equally likely outcomes, which may be then statistically evaluated, analogous to the discrete case of Eq. (1).

The algorithm used to obtain the set of equally likely design storm model outcomes is comprised of four sections. Section 1 describes how the error realizations are obtained from the model output (i.e., in prediction mode,) and the observed stream gauge information. Section 2 described how numerical approximation to the Volterra Integral is used to derive the error transfer function realizations. Section 3 describes how a design storm model is analyzed using the set of error transfer function realizations obtained in Section 2. The result is in Section 4, a set of equally likely runoff hydrograph outcomes.

MATHEMATICAL MODEL DEVELOPMENT

Section 1. The Error Realization

Reference to Fig. 1 shows how the observed stream gauge data (1.1) and the model output (1.2), for a given storm event, are subtracted to form the error realization (1.3) for the particular model under investigation. The error realization is denoted by $\xi_k^i(\cdot)$, where $i = 1, 2, 3, \dots, n$ is a particular two-hour interval, $k = 1, 2, 3, \dots, 6$ is the model under investigation, and (\cdot) is time. As shown in step 1.3, the error realization is obtained by subtracting the observed stream gauge data $Q_k(\cdot)$ at a particular time for the cumulative storm from the corresponding model output $M_k(\cdot)$ at that time, resulting in $M_k(\cdot) - Q_k(\cdot)$. Observed low flows measured at the gauge were not included, and so model base flow estimates did not affect the results.

Additional error data may be synthetically generated from the extracted data by using the Bootstrap method as described by Efron and Tribshirani (1993).

Section 2. Error Transfer Function Realizations

The second section of the algorithm depicts how an error transfer function realization $\psi_k^i(\cdot)$ is synthesized by using the inverse of the convolution procedure (Hromadka and Whitley, 1989). The convolution procedure is based on the Volterra Integral:

$$\xi_k^i(t) = \int_{s=0}^t M(t-s) \psi_k^i(s) ds \quad (2)$$

where s and t span the two-hour time intervals and $M(\cdot)$ is the two hour duration segment of the hydrologic model output under investigation. Although Eq. (2) defines the transfer function as determined from modeling estimates, an underlying assumption is that the resulting synthesized transfer functions are equally likely realizations from a stochastic process. It is noted that the synthesized transfer function is uniquely determined and has both positive and negative values (Hromadka and Whitley, 1989), so long as $M(\tau)$ and $\xi_k^i(\tau)$ begin to have nonzero values simultaneously. For example, Tsokos and Padgett (1974) develop in detail the use of stochastic integral equations to model the uncertainties inherent in biological processes as a Volterra Integral representation of data obtained by instrumentation and other measurements. In our case, the uncertainty in runoff estimates is modeled as a Volterra Integral representation of rainfall-runoff modeling estimates. The Volterra Integral may be approximated by use of the discrete convolution method. The convolution model for the algorithm is:

$$\xi_k^i(\cdot) = M_k^i(\cdot) \otimes \psi_k^i(\cdot) \quad (3)$$

where \otimes is notation for the convolution process of equation (2). In equation (3), the error realization $\xi_k^i(\cdot)$ is known from the supplied data, and the hydrologic model output $M_k^i(\cdot)$ is known. As before, $i = 1,2,3,\dots,n$. The underpinnings of Eq. (3) is to represent a particular rainfall-runoff model's history of performance (i.e., modeling error) as a stochastic process. In order to describe the stochastic process, a discrete set of realizations is used as a simple random sample, which is then bootstrapped to evolve a synthetic population. Obviously should a significant data

supply exist, those data should be used instead of synthetic data. However, it is recalled that only the errors resulting from validation tests should be used in Eqs. (1) to (3).

To solve for the error transfer function $\psi_k^i(\cdot)$, it will be necessary to re-write Eq. (3). For notational purposes, we will use the figure \odot to denote the inverse of the convolution procedure, so that:

$$\psi_k^i(\cdot) = M_k^i(\cdot) \odot \xi_k^i(\cdot) \quad (4)$$

where $\xi_k^i(\cdot)$ is the modeling error realization developed in equation (3). By numerically integrating Eq. (4) with respect to a two-hour duration and 5-minute unit intervals, Eq. (4) may be solved using linear algebra by re-stating $M_k^i(\cdot)$ as a square (24x24) matrix and $\xi_k^i(\cdot)$ as an (24x1) column vector. The situation where there is no solution to the inverse problems occurring when the first model value input is zero is handled within the computer program that was created. The resultant error transfer function realization $\psi_k^i(\cdot)$ will be in the form of an (24x1) column vector where $i = 1, 2, 3, \dots, n$. For $i = 1$, the first two hour duration segment of the combined $M_k^i(\cdot)$ is analyzed, resulting in the error transfer function realization $\psi_k^1(\cdot)$. For $i = 2$, the time interval is shifted to encompass the interval starting at $t = 5$ and ending at $t = 2$ hours plus five minutes. Again, the extracted error $\xi_k^2(\cdot)$ is used to determine the error transfer function realization $\psi_k^2(\cdot)$. For $i = 3$, the time base is again shifted to span the time interval starting at $t = 10$ minutes and ending at $t = 2$ hours plus 10 minutes. The process of incrementing the time base by five minutes and extracting the error transfer function realization for the included two-hour segment is repeated for the length of the combined storm duration, $M_{k1}(\cdot)$. The result will be set $\{\psi_k^i\}$ of synthetic, yet plausible, error transfer function realizations.

To expand the discrete set of transfer functions into a larger sampling domain, bootstrapping is used. The bootstrap method consists of randomly selecting a transfer function from the set of transfer functions, with replacement. Selection with replacement means that each time a transfer function is selected, the selection is made from the entire set, regardless of how many times each function has been selected previously, i.e. each function has the same probability of being selected. Naturally, bootstrapping sampling is a weak substitute for actual

data. However in this paper, bootstrapping provides a synthetic yet plausible population for use in statistical analysis.

Section 3. A Design Storm Prediction Model Evaluation

The third section of the algorithm incorporates the set of error transfer function realizations developed in Section 2. These transfer function realizations will be used to evaluate a rainfall-runoff model prediction, called the design storm model M_k^d (see step 3.1).

By re-arranging the formulation shown in step 1.3,

$$[Q(\cdot)]_k^d = M_k^d(\cdot) - [\xi(\cdot)]_k^d \quad (5)$$

as in step 3.2, $[Q]_k^d$ is the distribution of runoff hydrographs, for model type k , for design storm event d ; $[\xi(\cdot)]_k^d$ is the distribution of error realizations, for model type k , in prediction mode, and $M_k^d(\cdot)$ is the model type k runoff hydrograph, for design storm event, d . For evaluation purposes, the error distribution for the design storm model will be estimated by the stochastic process, in discrete form,

$$[\xi(\cdot)]_k^d \equiv M_k^d(\cdot) \otimes \{\psi_k^i(\cdot)\} \quad (6)$$

where $\{\psi_k^i(\cdot)\}$ is the set of error transfer function realizations obtained in Section 2. Equation (6) generates an ensemble of error realizations $[\xi(\cdot)]_k^d$ which are based on the error transfer function realizations developed for model type k discussed in sections 1 and 2, and here are convoluted with the design storm model output, $M_k^d(\cdot)$. For the design storm model, this step constitutes the transition from a single storm observation to a discrete statistical sample space capable of statistical analysis described in Section 4.

Equation (5) may then be re-written in terms of a stochastic process as:

$$[Q(\cdot)]_k^d = M_k^d(\cdot) - (M_k^d(\cdot) \otimes \{\psi_k^i(\cdot)\}) \quad (7)$$

for $i = 1,2,3,\dots,n$, where $[Q(\cdot)]_k^d$ is the stochastic process of equally likely outcomes for the design storm model d , and where as before, $k = 1,2,3,\dots,6$.

Section 4. Statistical Analysis of the Stochastic Process $[Q(\cdot)]_k^d$

The output of the algorithm, $[Q(\cdot)]_k^d$, consists of a discrete distribution of equally likely outcomes for the particular design storm prediction under consideration. Since we assume each outcome is equally likely, statistical methods may be used to obtain useful information from the results of the algorithm such as:

- 1) the maximum value of the model output (i.e., peak flow rate);
- 2) the expected value of the peak flow rate;
- 3) the median value of the peak flow rate estimates;
- 4) the variance of the peak flow rate estimates (the variance is particularly interesting, since it calls attention to the distribution, or spread, of the outcomes of each model under consideration);
- 5) confidence intervals, which would establish an interval that includes the true value of the peak flow rate with a pre-determined degree of certainty;
- 6) total runoff volume.

Other statistics may be similarly analyzed such as runoff volume, depth-duration characteristics, among others. The algorithm may be used to generate statistical data for each of the k models under consideration. Since the data are based on the error realizations obtained in Section 1, the output of the algorithm will reflect the actual discrepancy between the observed stream gauge data and the model under study, when applied in prediction model. (Of course, an additional increase in variance will occur in transposing the model sets to watersheds that are not part of the rainfall-runoff data set.)

By using the algorithm, it is possible to rank the six models under evaluation with respect to a statistical measure, such as the mean, for each $[Q(\cdot)]_k^d$.

APPLICATION

As described in the previous development, the actual rainfall-runoff model output is used in the stochastic integral equation in developing the stochastic process of runoff hydrographs in prediction mode. It is recalled that the error transfer function is defined by a set of equally likely realizations synthesized by equating a particular rainfall-runoff model output, in prediction mode (i.e., in this case, from validation tests), to the modeling error. That is, once the rainfall-runoff model is calibrated, the model is tested using known rainfall-runoff data that was not part of the calibration data set, resulting in realizations of modeling error for the given model in prediction mode. This approach describes the modeling error trends more appropriate to as applied in practice, rather than modeling error in matching its own calibration data.

In order to compare the above cited six rainfall-runoff models in relative performance, three hypothetical design storm runoff hydrographs are defined, labeled as A, B, and C. For output A, as an example, it is assumed that all six rainfall-runoff models have produced an output realization (runoff hydrograph) that is identical to the hypothetical realization, A. Then, the realization, A, is used in each of the respective stochastic integral representations to develop the distribution of runoff predictions.

As described above, six rainfall-runoff hydrological models, in prediction mode, were each compared to observed stream gauge data (from the model validation data set) at discrete time intervals and a set of error realizations was obtained for each of the six models. A set of error transfer function realizations $\{\psi_k\}$ was obtained for each of the six models, $k = 1, 2, \dots, 6$. The results may be seen in Figs. 2a-f, where the error transfer function realizations $\{\psi_k\}$ are plotted for the chosen two-hour time durations.

Each of the six hydrological models were used in conjunction with the three design storms to generate a set of probable design storm runoff hydrographs as shown in Figures 3a-f, 4a-f, and 5a-f. In each of the six figures (for each case of A, B, and C), the discrete statistical sample space is indicated by the dark plots, and the actual design storm prediction (i.e. A, B, or C) is shown by the white line seen within the shaded area.

Figures 6 through 11 show how the frequency distribution for design storm prediction A varies in accordance with the peak flow rate. The data are plotted in histogram form, so that the distribution of the design storm prediction for case A, for each of the six hydrological models, may be directly compared to the actual value.

As suggested in Section 4, Tables 1, 2, and 3 list the actual values for the peak flow rate and then list the mean and standard deviation for the peak flow rate of each of the six rainfall-runoff hydrological models as applied to each of the three design storm runoff hydrographs. Further, the tables list the actual total runoff volume and then list the mean and standard deviation for the total runoff volume for each of the six rainfall-runoff hydrological models as applied to each of the three design storm runoff hydrographs.

Table 1. Statistical Summary of Peak Flow Rate Values,
for Design Storm Runoff Hydrograph A

<u>Actual Value</u>			<u>HEC1</u>	<u>HSP</u>	<u>MITCAT</u>	<u>SSARR</u>	<u>STORM</u>	<u>SWMM</u>
748	Peak Q	Mean:	719	854	686	679	726	787
		Standard Deviations:	293	337	312	454	313	354
168	Volume	Mean:	160	190	154	152	165	179
		Standard Deviations:	72	73	74	92	76	78

Table 2. Statistical Summary of Peak Flow Rate Values,
for Design Storm Runoff Hydrograph B

<u>Actual Value</u>			<u>HEC1</u>	<u>HSP</u>	<u>MITCAT</u>	<u>SSARR</u>	<u>STORM</u>	<u>SWMM</u>
292	Peak Q	Mean:	284	334	264	262	274	305
		Standard Deviations:	105	136	119	209	115	158
37	Volume	Mean:	37	43	36	35	38	42
		Standard Deviations:	16	17	16	22	16	18

Table 3. Statistical Summary of Peak Flow Rate Values,
for Design Storm Runoff Hydrograph C

<u>Actual Value</u>			<u>HEC1</u>	<u>HSP</u>	<u>MITCAT</u>	<u>SSARR</u>	<u>STORM</u>	<u>SWMM</u>
648	Peak Q	Mean:	640	757	613	604	64	714
		Standard Deviations:	247	318	280	484	267	381
95	Volume	Mean:	98	113	94	91	99	108
		Standard Deviations:	40	42	42	55	42	46

In examining Figs. 3, 4, and 5, it is seen that for all six rainfall-runoff models, there is a considerable dispersion in prediction results. Generally, the vast majority of probable prediction hydrographs have a shape that emulate the original rainfall-runoff model output. However from the figures, there are occurrences of significantly delayed peak flows that reflect similar occurrences observed from the historic performance data of these models in the tests performed by Abbott (1978). That is, the realizations shown in the figures reflect the history of rainfall-runoff model performance as noted in validation tests.

In our case, the stochastic process shown in Figs. 2, 3, 4, and 5 reflect the use of bootstrapping in order to populate the low population discrete distribution of the original data. If validation results were to be preserved by the engineering community in a common data base, for all rainfall-runoff models, then bootstrapping would not be needed as sufficient performance data would exist.

It is noted, that the results reflect the variance in modeling estimates as developed from validation results. In practice, one generally does not have a calibrated rainfall-runoff model on a site by site basis, but may have a regionally calibrated model. This occurrence will result in less certainty in modeling results, and there will be a corresponding increase in the variance in prediction results addressed herein. To study this later effect, the approach described above can be readily extended to develop error realizations from site uncalibrated rainfall-runoff models versus stream gauge data, and the corresponding stochastic integral equation formulation is developed analogously.

The objective evaluation based on error realizations may be used as a comparative tool to rank as set of hydrologic models under consideration. For example, reference to Tables 1, 2, and 3 shows that, for the three design storm runoff hydrograph test cases, ranking the six hydrologic models with respect to how accurately their expected value estimates predict the peak flow rate (for the considered test cases of Abbott, 1978) yields the following order:

Table 4. Ranking of Rainfall-Runoff Model Predictions of Peak Flow Rate Expected Values

<u>Case A</u>	<u>Case B</u>	<u>Case C</u>
1) STORM	1) HEC1	1) HEC1
2) HEC1	2) SWMM	2) STORM
3) SWMM	3) STORM	3) MITCAT
4) MITCAT	4) MITCAT	4) SSARR
5) SSARR	5) SSARR	5) SWMM
6) HSP	6) HSP	6) HSP

Similarly, the six hydrologic models may be ranked with respect to how accurately their expected value estimates predict the total runoff volume.

Table 5. Ranking of Rainfall-Runoff Model Predictions of Peak Flow Rate of Runoff Volume Expected Values

<u>Case A</u>	<u>Case B</u>	<u>Case C</u>
1) STORM	1) HEC1	1) MITCAT
2) HEC1	2) MITCAT, STORM	2) HEC1
3) SWMM	3) SSARR	3) SSARR, STORM
4) MITCAT	4) SWMM	4) SWMM
5) SSARR	5) HSP	5) HSP
6) HSP		

As for dispersion of predicted estimates, however, the standard deviation of prediction results rank as shown in Tables 6 and 7.

Table 6. Ranking of Rainfall-Runoff Model Predictions of Peak Flow Rate Standard Deviation

<u>Case A</u>	<u>Case B</u>	<u>Case C</u>
1) HEC1	1) HEC1	1) HEC1
2) MITCAT	2) STORM	2) STORM
3) STORM	3) MITCAT	3) MITCAT
4) HSP	4) HSP	4) HSP
5) SWMM	5) SWMM	5) SWMM
6) SSARR	6) SSARR	6) SSARR

Table 7. Ranking of Rainfall-Runoff Model Predictions of Runoff Volume Standard Deviation

<u>Case A</u>	<u>Case B</u>	<u>Case C</u>
1) HEC1	1) HEC1	1) HEC1
2) HSP	2) MITCAT	2) HSP
3) MITCAT	3) STORM	3) MITCAT
4) STORM	4) HSP	4) STORM
5) SWMM	5) SWMM	5) SWMM
6) SSARR	6) SSARR	6) SSARR

CONCLUSIONS

Sections 1 through 4 show how a stochastic process has been developed that objectively evaluates rainfall-runoff hydrologic model performance in prediction mode. The process relies solely on data which the hydrologic models themselves produce in validation tests where calibrated rainfall-runoff models are tested against rainfall-runoff data sets not included in the calibration data sets. The runoff hydrographs from the rainfall-runoff hydrologic model, in prediction mode, is compared to the corresponding stream gauge data obtained during the same storm event. The deviation between the two realizations is recorded as an error realization (Section 1).

A convolution procedure (based on the Volterra Integral) is used to obtain a set of error transfer function realizations using the storm model output and the error realizations (Section 2). The algorithm may now be used to statistically evaluate a design storm model runoff hydrograph prediction.

The algorithm is used to generate a synthetic set of error transfer function realizations, but here the error realization is obtained by the convolution of the design storm model output and the previously generated error transfer functions. This produces an ensemble of design storm error realizations (Section 3). The error realizations are then subtracted from the design storm model result to obtain a set of equally likely outcomes for the design storm model. This statistical information is based solely on the error realizations obtained from the models themselves, in prediction mode.

The work of Tsokos and Padgett (1978) demonstrates the predictive ability available by use of a stochastic integral equation such as Eq. (2). However, further research is needed to demonstrate the predictive ability of Eq. (2) in rainfall-runoff modeling. Perhaps model users could make available their validation/calibration data sets of stream gauge data and model results via the internet. In time, a considerable data set "history" of model performance would be assembled and subsequently could be analyzed using a stochastic integral equation formulation such as presented herein. Further research is also needed regarding issues of "filtering" the error distribution such as to avoid so-called "negative runoff". Obviously, the presented results could have been filtered so as to present a more

tractable appearance; however, by presenting a non-filtered set of results, a more accurate representation of the modeling results is presented.

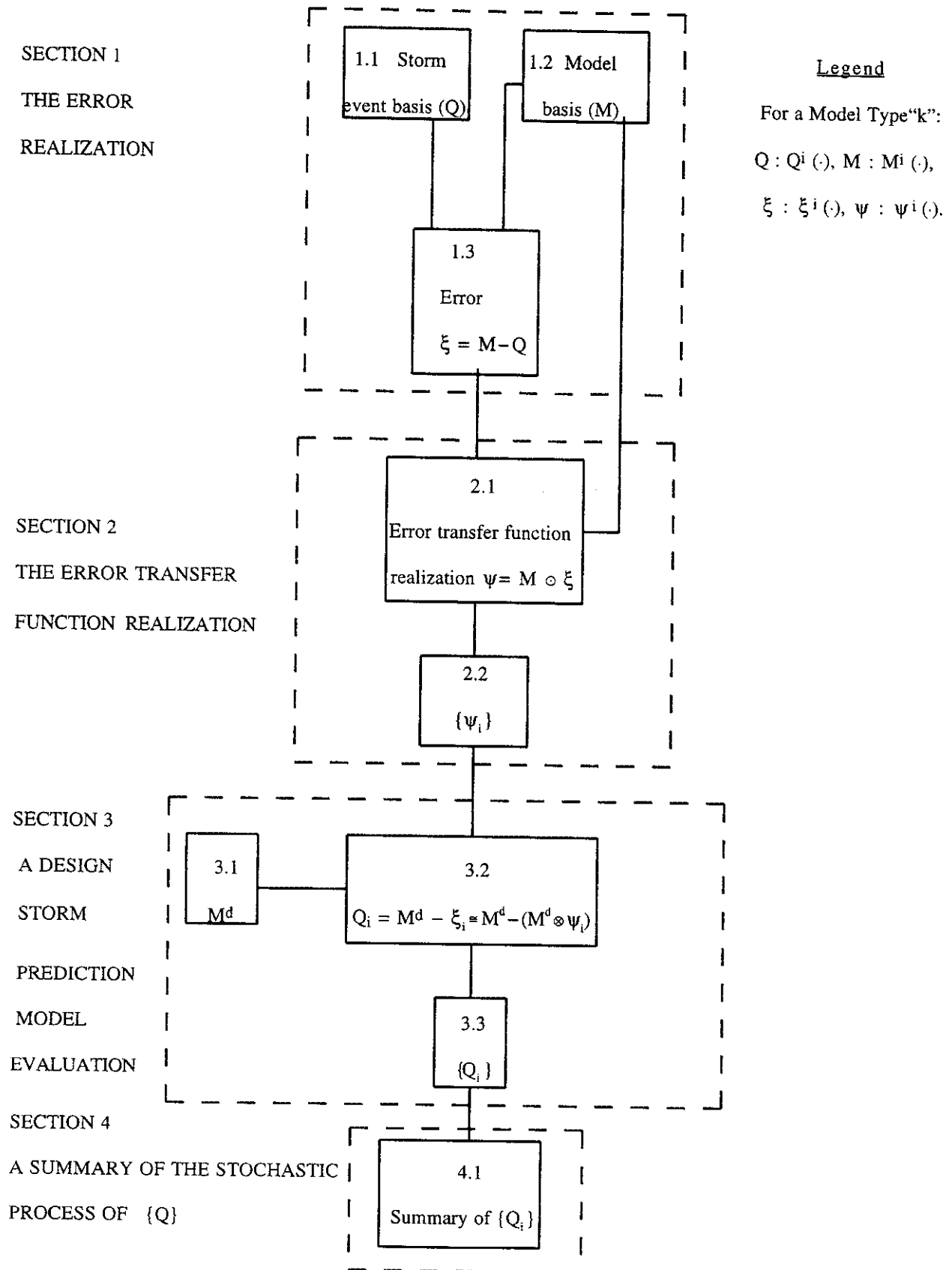
REFERENCES

1. Efrom, B., and R.J. Tribshirani, An Introduction to the Bootstrap, Chapman and Hall, 1993.
2. Hromadka II, T.V., R.H. McCuen, and C.C. Yen, Computational Hydrology in Flood Control Design and Planning, Lighthouse Publications, pp. 28-33, 1987.
3. Hromadka II, T.V., and R.J. Whitley, Stochastic Equations and Rainfall-Runoff Models, Springer-Verlag, p. 86, 1989.
4. Tsokos, C.P. and W.J. Padgett, Random Integral Equations with Applications to Life Science and Engineering, Academic Press, 1974.
5. Abbott, Jess, U.S. Army Corps of Engineers, The Hydrologic Engineering Center, "Testing of Several Runoff Models on an Urban Watershed," Technical Paper No. 59, 1978.

LIST OF FIGURES

- Figure 1. An Algorithm for Statistically Evaluating Rainfall-Runoff Model Prediction Performance.
- Figure 2. The Stochastic Process of Error Transfer Functions for Each Rainfall-Runoff Model.
- Figure 3. The Stochastic Process of Runoff Hydrographs, for Each Rainfall-Runoff Model, for Design Storm Runoff Hydrograph A (shown in white).
- Figure 4. The Stochastic Process of Runoff Hydrographs, for Each Rainfall-Runoff Model, for Design Storm Runoff Hydrograph B (shown in white).
- Figure 5. The Stochastic Process of Runoff Hydrographs, for Each Rainfall-Runoff Model, for Design Storm Runoff Hydrograph C (shown in white).
- Figure 6. Frequency Distribution Plot of Peak Q Predictions for Case A, for the HEC-1 Model.
- Figure 7. Frequency Distribution Plot of Peak Q Predictions for Case A, for the HSP Model.
- Figure 8. Frequency Distribution Plot of Peak Q Predictions for Case A, for the MITCAT Model.
- Figure 9. Frequency Distribution Plot of Peak Q Predictions for Case A, for the SSARR Model.
- Figure 10. Frequency Distribution Plot of Peak Q Predictions for Case A, for the STORM Model.
- Figure 11. Frequency Distribution Plot of Peak Q Predictions for Case A, for the SWMM Model.

Fig. 1 An algorithm for statistically evaluating rainfall-runoff model prediction performance.



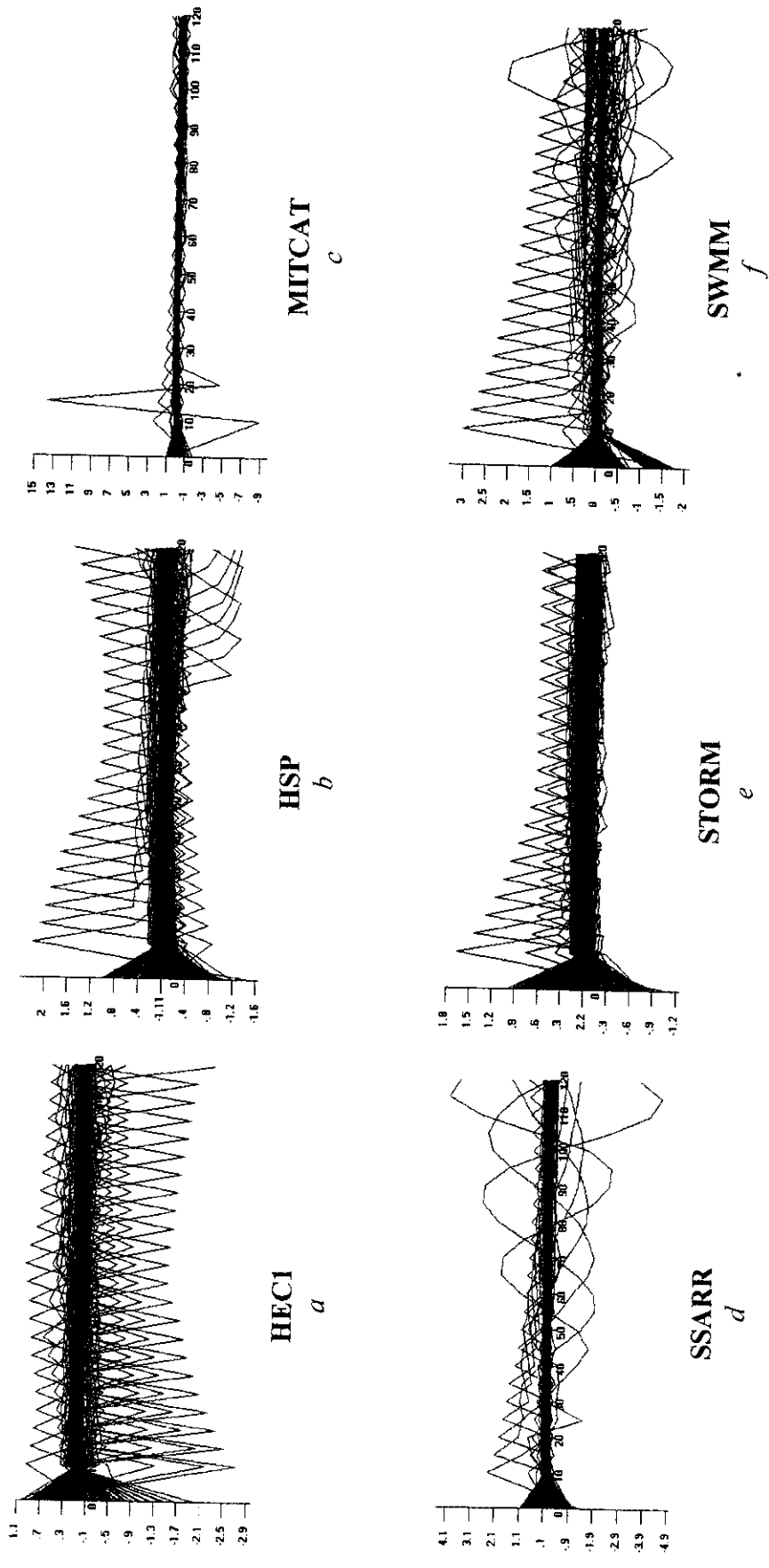


Figure 2. The stochastic process of error transfer functions for each rainfall-runoff model.

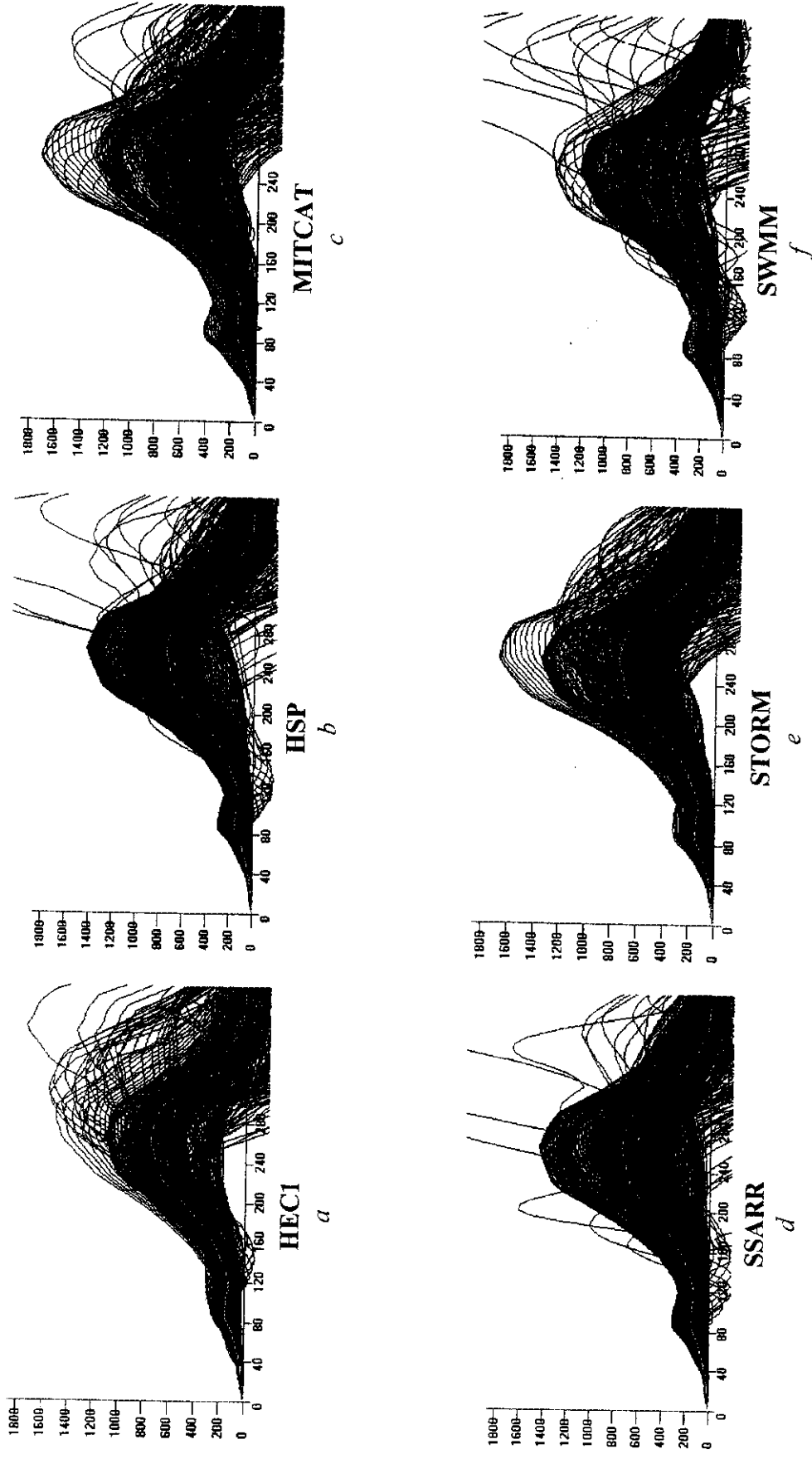


Figure 3. The stochastic process of runoff hydrographs, for each rainfall-runoff model, for design storm runoff hydrograph A (shown in white)

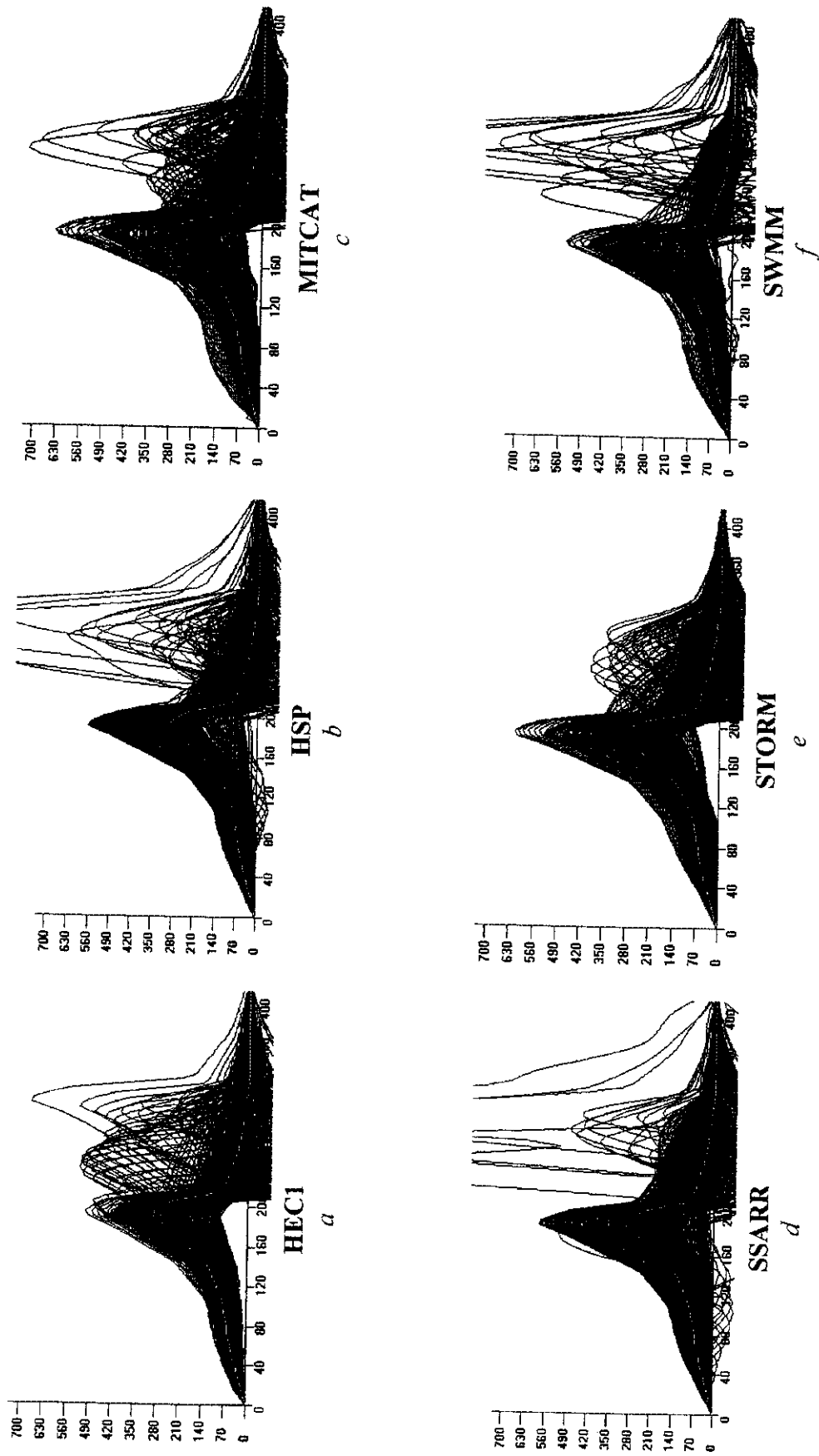


Figure 4. The stochastic process of runoff hydrographs, for each rainfall-runoff model, for design storm runoff hydrograph B (shown in white)

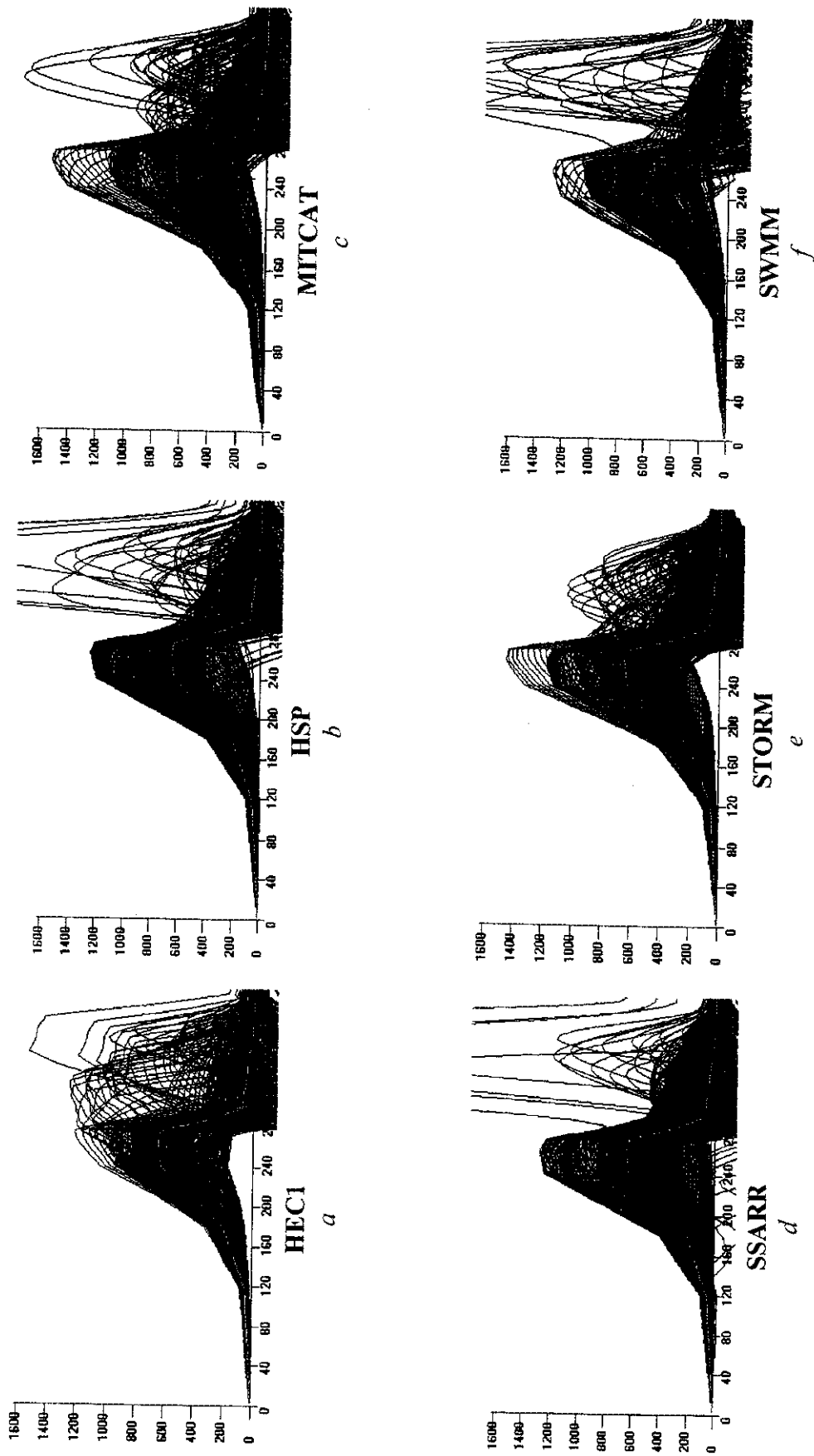


Figure 5. The stochastic process of runoff hydrographs, for each rainfall-runoff model, for design storm runoff hydrograph C (shown in white)

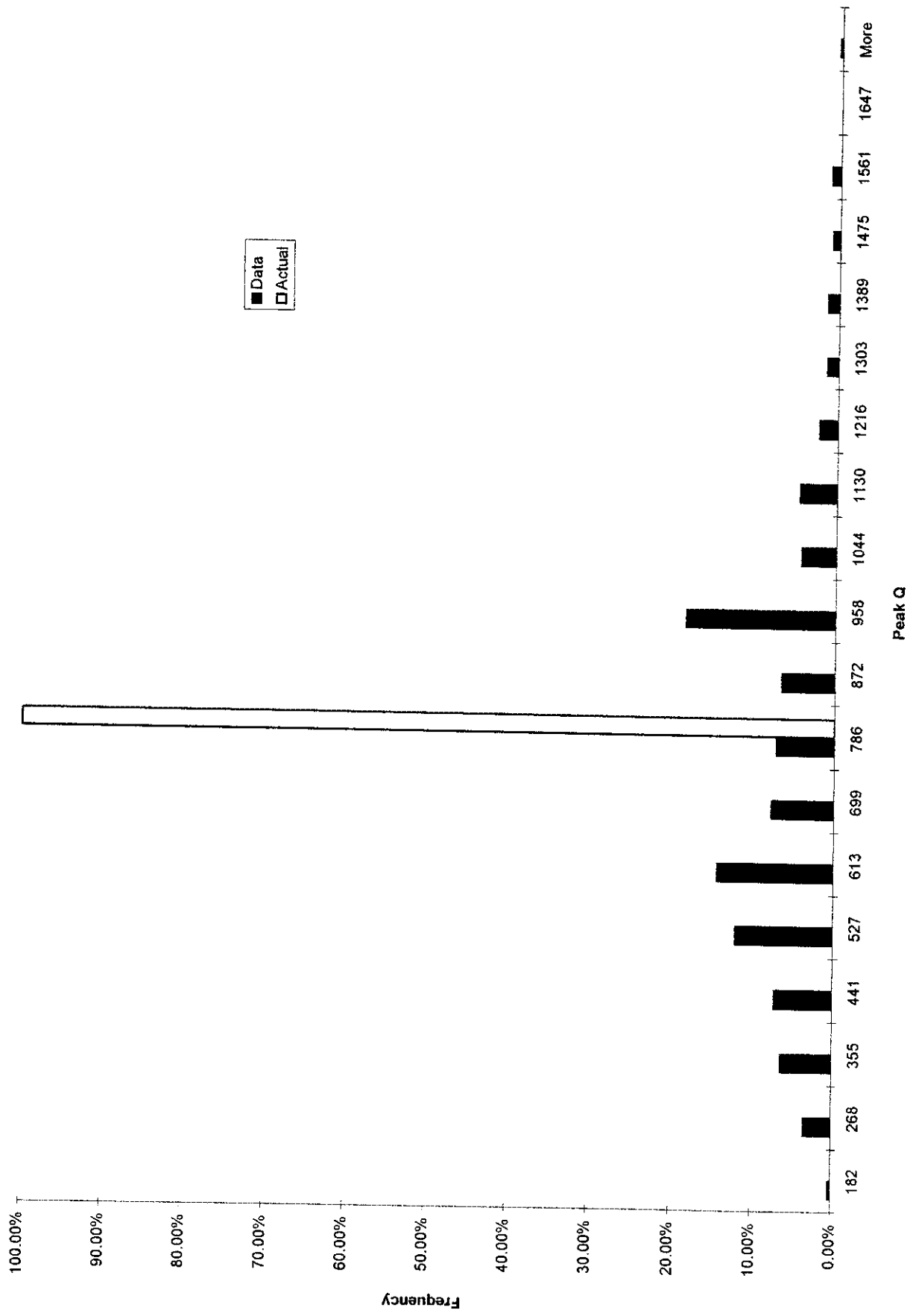


Figure 6. Frequency Distribution Plot of Peak Q Predictions for Case A, for the HEC-1 Model.

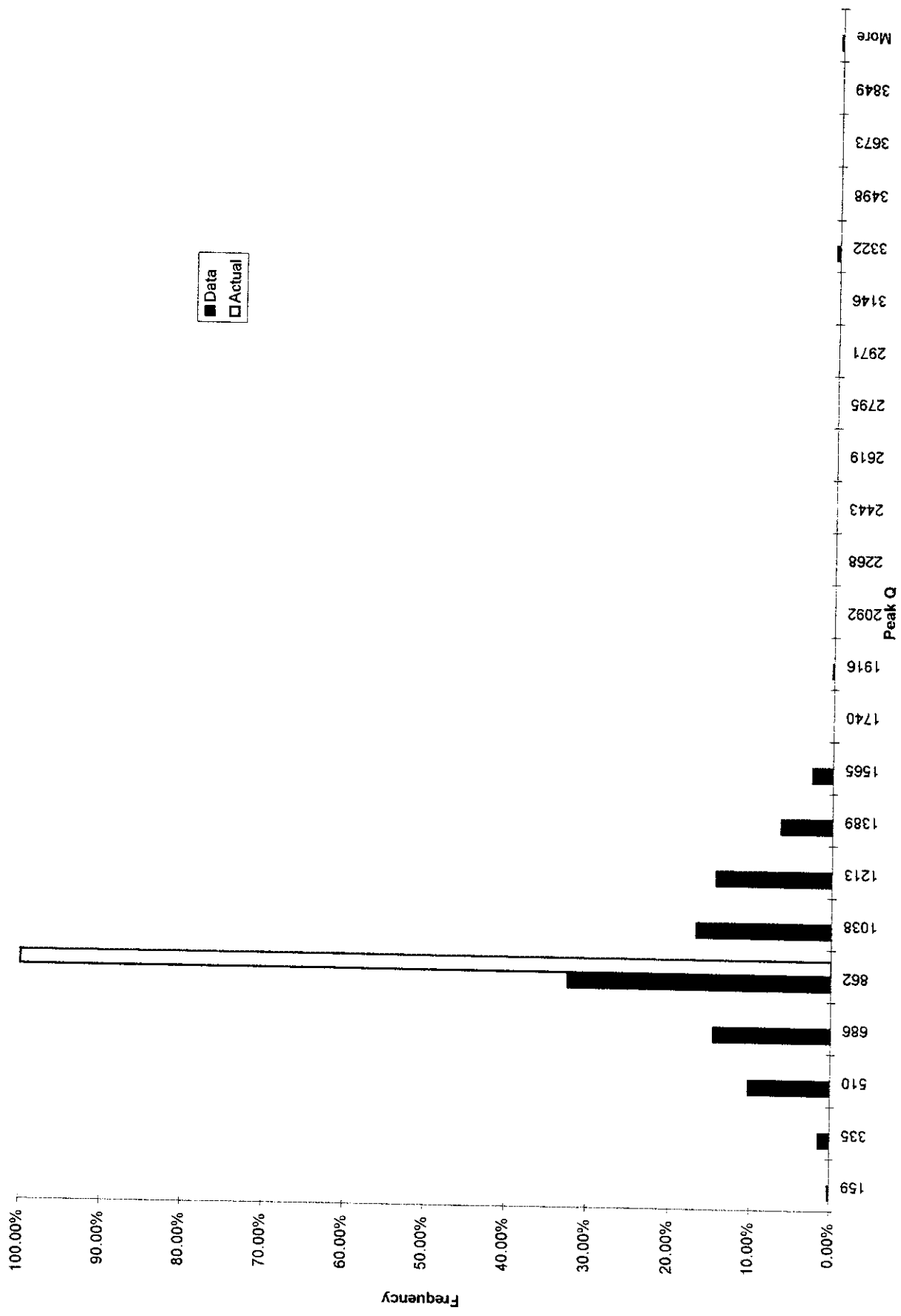


Figure 7. Frequency Distribution Plot of Peak Q Predictions for Case A, for the HSP Model.

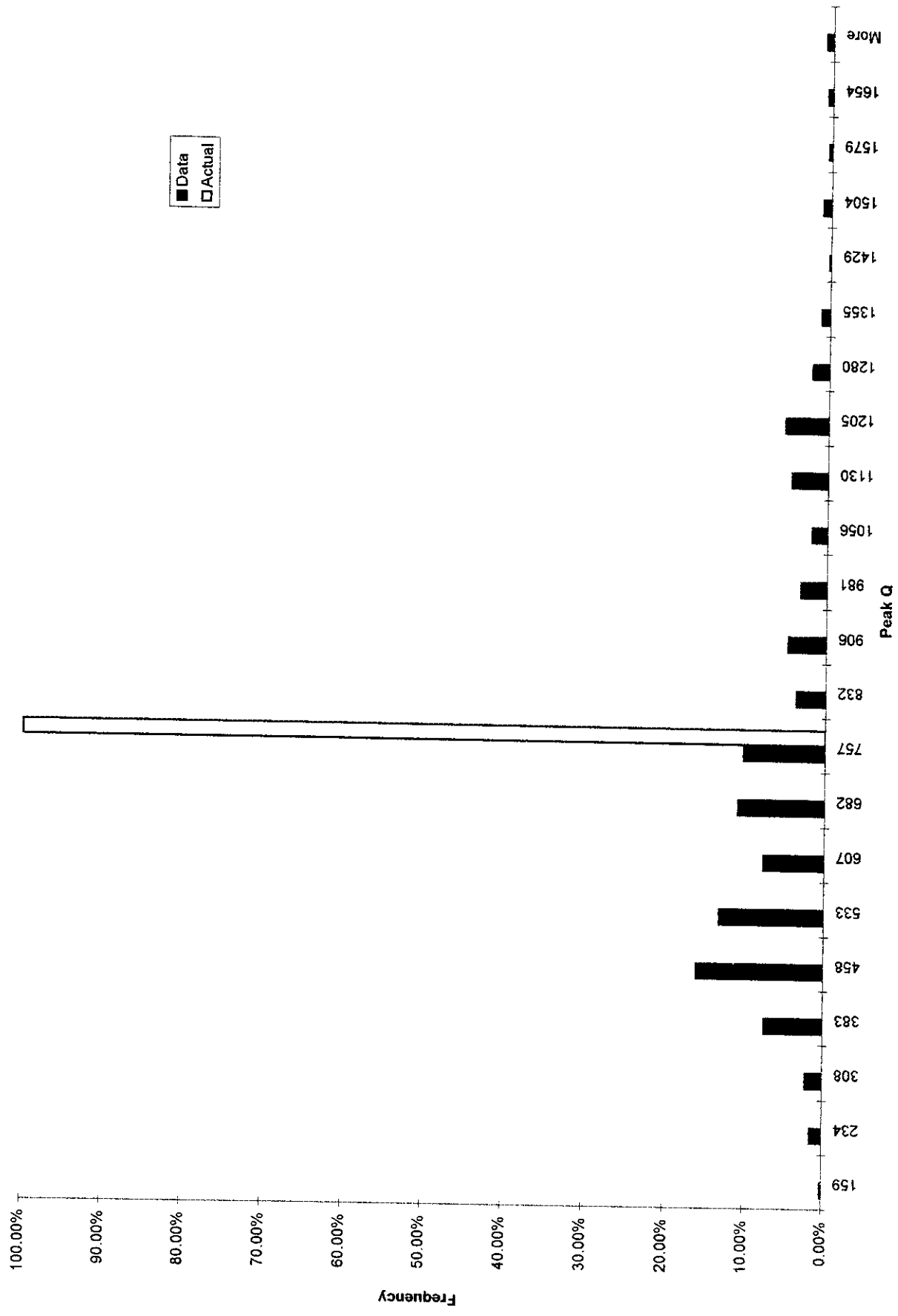


Figure 8. Frequency Distribution Plot of Peak Q Predictions for Case A, for the MITCAT Model.

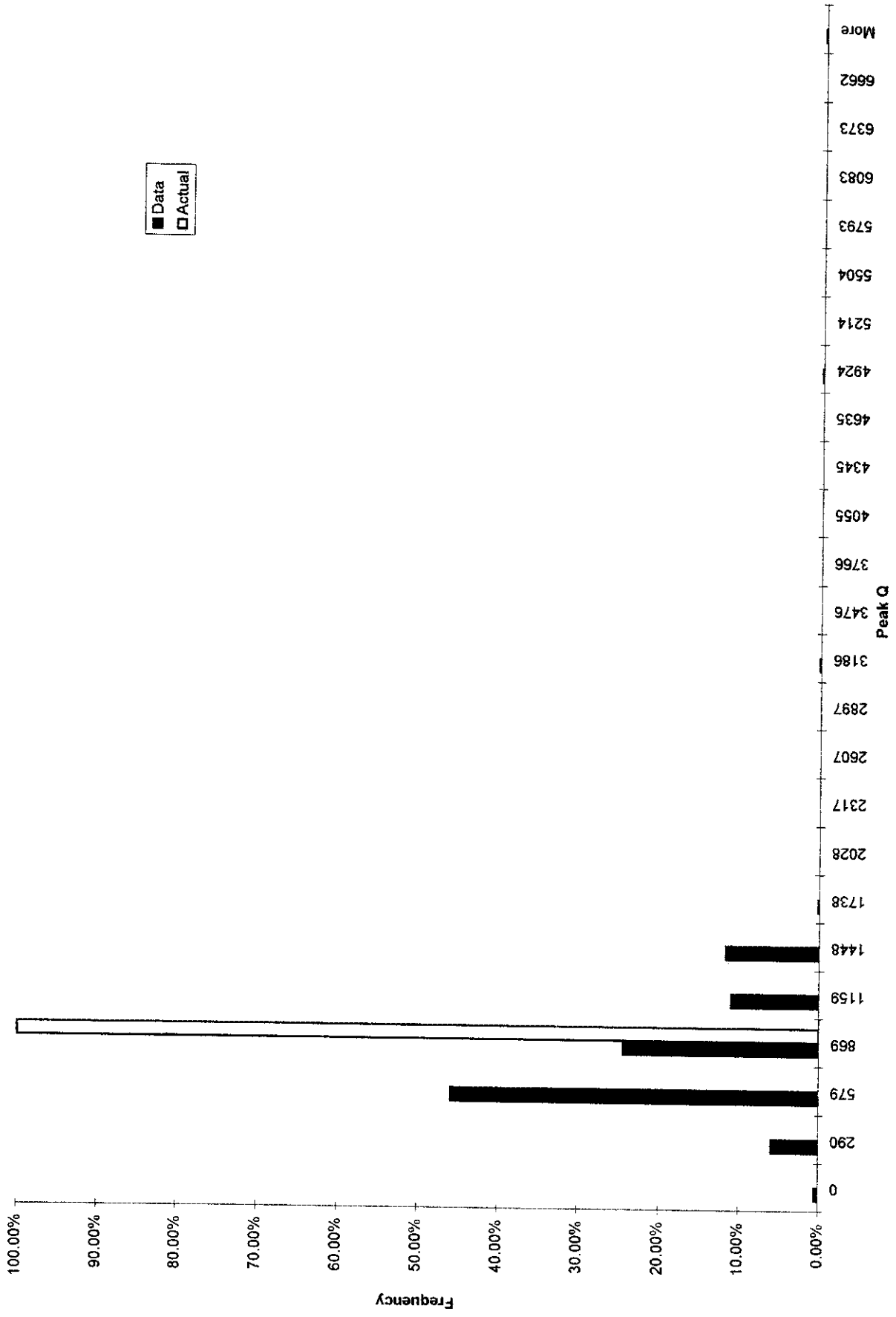


Figure 9. Frequency Distribution Plot of Peak Q Predictions for Case A, for the SSARR Model.

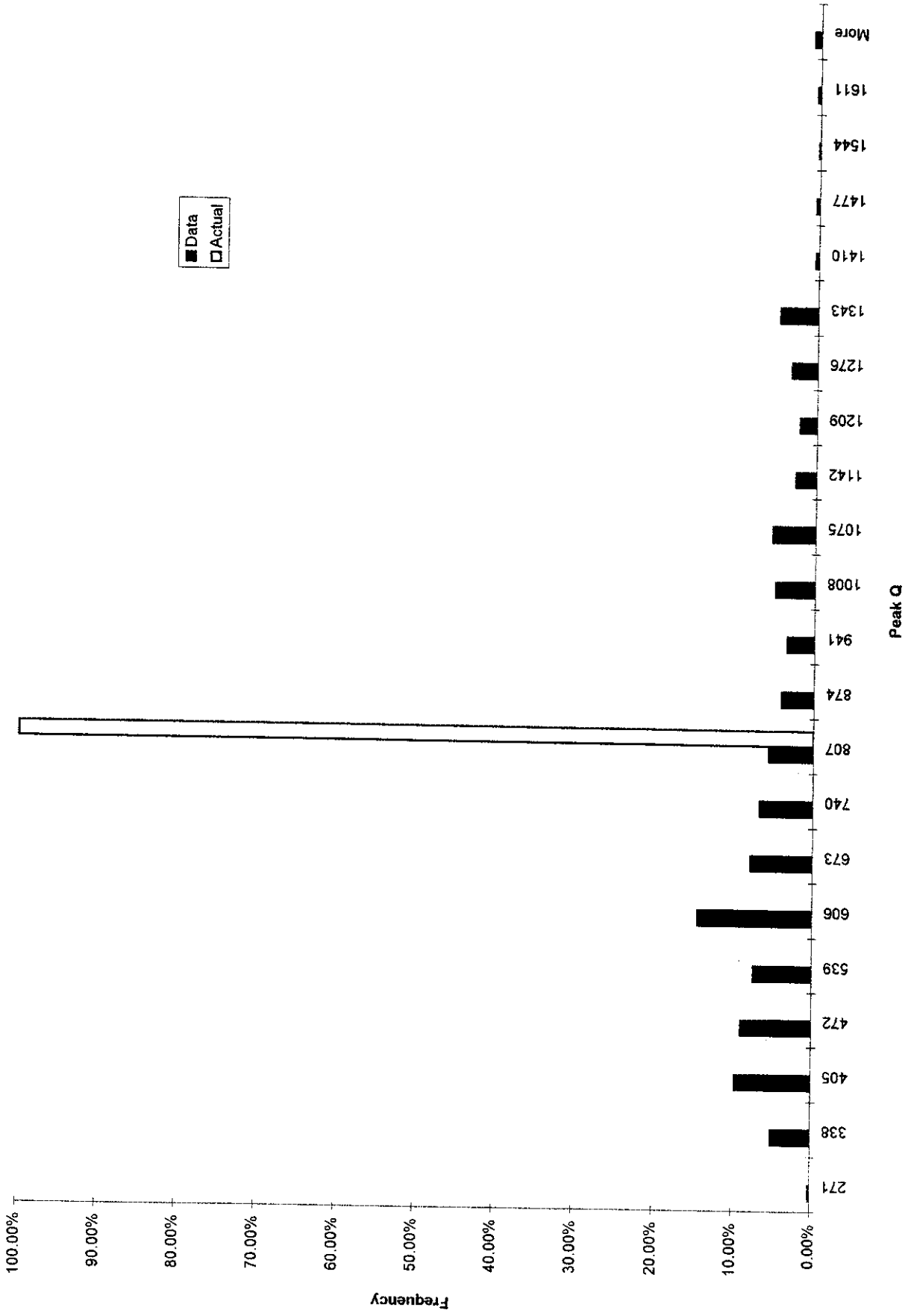


Figure 10. Frequency Distribution Plot of Peak Q Predictions for Case A, for the STORM Model.

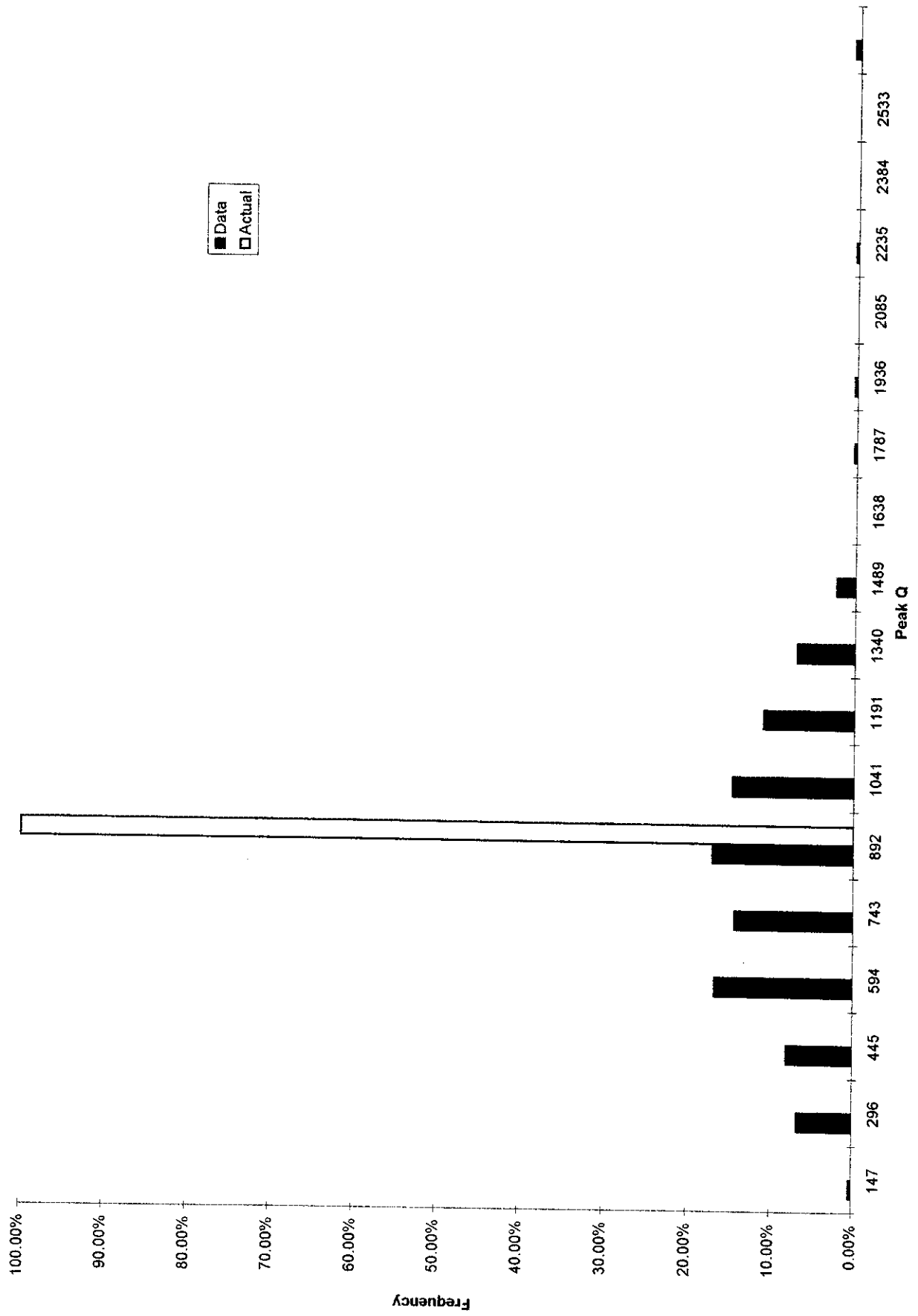


Figure 11. Frequency Distribution Plot of Peak Q Predictions for Case A, for the SWMM Model.